Is a quantum standing wave composed of two traveling waves?

B. W. Shore

Theoretical Atomic and Molecular Physics Group, Lawrence Livermore National Laboratory, Livermore, California 94550

P. Meystre and S. Stenholm*

Optical Sciences Center, University of Arizona, Tucson, Arizona 85721

Received April 19, 1990; accepted August 29, 1990

We compare the scattering of an atom by two different quantized standing-wave configurations. The first one is established in a cavity by a pair of fixed mirrors. The other consists of two independent counterpropagating traveling waves, as could occur in a ring configuration. We show that in the quantum regime (of small photon numbers) atoms are scattered differently by a true standing wave than by a superposition of two counterpropagating waves of equal amplitudes and opposite directions. This behavior is a manifestation of momentum conservation. In the case of traveling waves each wave depletes its momentum independently, whereas the standing wave that is fixed in space acts as a potentially infinite sink or source for momentum.

1. INTRODUCTION

The deflection of atoms in light fields is a subject of considerable current interest,[1] in particular in connection with the potential realization of atom interferometers.[2,3] Previous experiments[4–10] have employed strong standing-wave fields. These can be described, to an excellent degree of approximation, as classical fields. However, advances in cavity quantum electrodynamics[11] may shortly permit atom scattering by few-photon standing-wave fields. It is therefore timely to consider the possibility that quantum-mechanical properties of the field will produce observable effects. In pursuing this question we are led to consider the difference between standing and running waves.

Both standing and traveling waves are routinely used as basis fields in creating a quantum theory of electrodynamics. The two different descriptions of fields give the same predictions for single-photon transition rates, such as spontaneous emission and photoionization. However, we show that in the quantum regime (of small photon numbers) atoms are scattered differently by a true standing wave than by a superposition of two counterpropagating waves of equal amplitudes and opposite directions. No such difference occurs classically.

To probe the field we consider a collimated stream of atoms that travel across the standing-wave pattern. With passing time the field induces absorption and emission of energy. The emission and absorption of radiation not only changes the atomic excitation energy but also alters the momentum of the atomic center of mass. Atoms undergo two types of momentum change as they cross a resonant standing wave. First, their transverse momentum spreads. Second, if the atoms cross the field at an angle, they undergo Bragg scattering from the periodic structure provided by the wave. Classically, this behavior can be understood in terms of traveling waves: The atom catalyzes the transfer of momentum from one traveling wave to the other, thereby changing its own transverse momentum. In the quantum regime, however, there is an essential difference between scattering by two running waves and by a standing wave. With running waves we can in principle know which of the two waves has exchanged a unit of momentum with the atom. In contrast, a standing wave is an inseparable quantum unit whose average momentum remains zero at all times. This unity is imposed by the fixed mirrors that establish the standing wave. These act as infinite sinks of momentum. The reasons for this difference are deeply rooted in the foundation of field quantization. Quantum mechanics forbids one even in principle to determine, by means of a field measurement, from which traveling wave the atom picked up its momentum. To demonstrate this point, we present the deflection of an atom both in a standing wave and in a superposition of two counterpropagating running waves.

To appreciate the mathematical distinction between standing and running waves, consider the positive frequency operator formed by the superposition of two counterpropagating plane waves:

$$\hat{\mathcal{A}}(x,t) = \alpha[\hat{a}_1 \exp(ikx) + \hat{a}_2 \exp(-ikx)]\exp(-i\omega t). \quad (1)$$

Here $\hat{a}_i$ and $\hat{a}_i^\dagger$ are the annihilation operators for the two running-wave modes, obeying the boson commutation relations $[\hat{a}_i, \hat{a}_j^\dagger] = \delta_{ij}$. Their action on the running-wave two-mode number state $|n_1, n_2\rangle_R$ is

$$\hat{a}_1|n_1,n_2\rangle_R = n_1^{1/2}|n_1-1,n_2\rangle_R,$$
$$\hat{a}_2|n_1,n_2\rangle_R = n_2^{1/2}|n_1,n_2-1\rangle_R. \quad (2)$$

Equation (1) may be reexpressed as

$$\hat{\mathcal{A}}(x,t) = 2^{1/2}\alpha[\hat{a}_c \cos(kx) + i\hat{a}_s \sin(kx)]\exp(-i\omega t), \quad (3)$$

0740-3224/91/040903-08$05.00

where

$$\hat{a}_c = 2^{-1/2}(\hat{a}_1 + \hat{a}_2), \qquad \hat{a}_s = 2^{-1/2}(\hat{a}_1 - \hat{a}_2). \tag{4}$$

The operators $\hat{a}_c$ and $\hat{a}_s$ also obey boson commutation relations, but they act on standing-wave modes rather than on traveling-wave modes; specifically,

$$\hat{a}_s|n_s, n_c\rangle_S = n_s^{1/2}|n_s - 1, n_c\rangle_S,$$
$$\hat{a}_c|n_s, n_c\rangle_s = n_c^{1/2}|n_s, n_c - 1\rangle_S, \tag{5}$$

and similarly for $\hat{a}_s^\dagger$ and $\hat{a}_c^\dagger$.

Although the choice of standing waves and running waves appears, in typical quantum experiments, to be a matter of mathematical convenience, it is possible to recognize a physical distinction. In one dimension, standing-wave basis fields are the natural choice when the field is contained within a cavity bounded by two mirrors. In particular, for perfectly reflecting mirrors one can chose the origin such that only one of the modes (say, the cosine-type mode) matches the electric-field boundary conditions for a given frequency. It is then possible to employ a single-mode description. Conversely, traveling waves are the natural choice when the field comprises counterpropagating beams confined to a ring by three mirrors. By maintaining counterpropagating fields of equal amplitude, one establishes in the ring configuration a stationary standing wave.

2. MODEL

We consider a two-state atom of mass M with internal excitation described by the ground and excited basis states $|-\rangle$ and $|+\rangle$, whose excitation energies are $-\hbar\omega_0/2$ and $\hbar\omega_0/2$, respectively. It interacts with a plane-wave monochromatic field of frequency ω that is linearly polarized along the y axis. The atom is assumed to propagate with momentum p_z predominantly in the z direction perpendicular to the light field. We neglect spontaneous emission and other incoherent processes, which are unessential for the present discussion, so that the atom–field behavior is governed by a time-dependent Schrödinger equation. We describe the evolution of the atom–field system in a reference frame moving at the constant velocity p_z/M; i.e., we neglect the field-induced changes of atomic velocity along the z axis and effectively treat p_z as a classical quantity.

When the atom interacts with a standing wave, the atom–field Hamiltonian is given in the dipole and rotating-wave approximations by[12]

$$H^s = \frac{1}{2M}\hat{p}^2 + \frac{1}{2}\hbar\omega_0\sigma_3 + \hbar\omega\hat{a}^\dagger\hat{a} + \frac{\hbar\Omega_0}{4}(\sigma_+\hat{a} + \sigma_-\hat{a}^\dagger)[\exp(ik\hat{x}) + \exp(-ik\hat{x})]. \tag{6}$$

Here $\hat{x}$ is the transverse position of the atomic center of mass, so that $[\hat{x}, \hat{p}] = i\hbar$. The factor Ω_0 in the coupling constant is the standing-wave vacuum Rabi frequency.[12] The operators σ_3, σ_+, and σ_- are defined by

$$\sigma_3|+\rangle = |+\rangle, \qquad \sigma_3|-\rangle = -|-\rangle,$$
$$\sigma_+|-\rangle = |+\rangle, \qquad \sigma_-|+\rangle = |-\rangle, \qquad \sigma_+|+\rangle = \sigma_-|-\rangle = 0. \tag{7}$$

The operators $\hat{a}$ and $\hat{a}^\dagger$ are the standing-wave mode annihilation and creation operators and obey the commutation relation $[\hat{a}, \hat{a}^\dagger] = 1$. (They are just the operators $\hat{a}_c$ and $\hat{a}_c^\dagger$ of Section 1.) Their action on the cosine standing-wave number state $|n\rangle$ is

$$\hat{a}|n\rangle = n^{1/2}|n - 1\rangle, \qquad \hat{a}^\dagger|n\rangle = (n + 1)^{1/2}|n + 1\rangle. \tag{8}$$

In contrast, the atom–field Hamiltonian for the case of two counterpropagating running waves is, for the same approximations,[13]

$$H = \frac{1}{2M}\hat{p}^2 + \frac{1}{2}\hbar\omega_0\sigma_3 + \hbar\omega(\hat{a}_1^\dagger\hat{a}_1 + \hat{a}_2^\dagger\hat{a}_2) + \frac{\hbar\Omega_0}{2(2)^{1/2}}\{\sigma_+[\hat{a}_1\exp(ik\hat{x}) + \hat{a}_2\exp(-ik\hat{x})] + \sigma_-[\hat{a}_1^\dagger\exp(-ik\hat{x}) + \hat{a}_2^\dagger\exp(ik\hat{x})]\}. \tag{9}$$

Note that the coupling constant for the running modes is larger than that for a standing mode by a factor of $2^{1/2}$, as is well known from field quantization procedures and can readily by inferred from the discussion in Section 1. Note also that we should not expect the situations described by the Hamiltonians of Eqs. (6) and (9) to be identical, since even the nature of the Hilbert spaces is different in the two cases. It takes two single-mode Fock spaces to describe two running waves, whereas a standing wave requires only one Fock space. This single space is a single, inseparable quantum system.

For the running-waves case, it is useful to apply the unitary transformation

$$U = \exp[-ik\hat{x}(\hat{a}_2^\dagger\hat{a}_2 - \hat{a}_1^\dagger\hat{a}_1)] \tag{10}$$

to the Hamiltonian of Eq. (9). Noting that $U\hat{a}_1U^\dagger = \exp(-ik\hat{x})\hat{a}_1$ and using the commutation relation $[\exp(-ik\hat{x}), f(\hat{p})] = f(\hat{p} + \hbar k)$, we readily obtain the transformed Hamiltonian

$$H^r = \frac{1}{2M}[\hat{p} - \hbar k(\hat{a}_1^\dagger\hat{a}_1 - \hat{a}_2^\dagger\hat{a}_2)]^2 + \frac{1}{2}\hbar\omega_0\sigma_z + \hbar\omega(\hat{a}_1^\dagger\hat{a}_1 + \hat{a}_2^\dagger\hat{a}_2) + \frac{\hbar\Omega_0}{2(2)^{1/2}}[\sigma_+(\hat{a}_1 + \hat{a}_2) + \sigma_-(\hat{a}_1^\dagger + \hat{a}_2^\dagger)]. \tag{11}$$

In the transformed Hamiltonian the exchange of momentum is no longer associated with the dipole interaction. Rather, the transformed kinetic energy explicitly accounts for momentum conservation.

3. EQUATIONS OF MOTION

Consider the effect on an atom of a standing wave. For concreteness, we assume that the atom is initially in its ground electronic state $|-\rangle$ with transverse kinetic momentum $p_z = p_0$. The Hilbert space of the system is the direct product of the Hilbert spaces for the field mode for the center of mass motion of the atom and for its internal degree of freedom. The basis states have the form $|\text{field, motion, internal}\rangle = |n, p, \pm\rangle$. Motivated by the fact that $\hat{a}^\dagger\hat{a} + \sigma_3/2$ is a constant of motion, we expand the state vector $|\Psi(t)\rangle$ of the combined atom–field system as

$$|\Psi(t)\rangle = \sum_{\nu,n} \exp(-i\omega n t)[C_{n,\nu}^{+}(t)\exp(-i\omega t/2)|n, p_0 + \nu\hbar k, +\rangle + C_{n,\nu}^{-}(t)\exp(i\omega t/2)|n, p_0 + \nu\hbar k, -\rangle], \quad (12)$$

with $n \geq 0$ and ν an integer. From the time-dependent Schrödinger equation, we obtain the equations of motion for the probability amplitudes:

$$i\hbar\frac{d}{dt}C_{n,\nu}^{-}(t) = \left[\frac{(p_0 + \nu\hbar k)^2}{2M} - \frac{1}{2}\hbar(\omega_0 - \omega)\right]C_{n,\nu}^{-}(t) + \frac{\hbar\Omega_0}{4}n^{1/2}[C_{n-1,\nu+1}^{+}(t) + C_{n-1,\nu-1}^{+}(t)] \quad (13)$$

and

$$i\hbar\frac{d}{dt}C_{n-1,\nu}^{+}(t) = \left[\frac{(p_0 + \nu\hbar k)^2}{2M} + \frac{1}{2}\hbar(\omega_0 - \omega)\right]C_{n+1,\nu}^{+}(t) + \frac{\hbar\Omega_0}{4}n^{1/2}[C_{n,\nu+1}^{-}(t) + C_{n,\nu-1}^{-}(t)]. \quad (14)$$

We have seen in Section 1 that, whereas the standing-wave case requires only one field mode, the running-waves case requires two modes. With the observation that $\hat{a}_1^{\dagger}\hat{a}_1 + \hat{a}_2^{\dagger}\hat{a}_2 + \sigma_3/2$ is now a constant of motion, and using the explicit momentum conservation apparent in the Hamiltonian of Eq. (11), we expand the state vector $|\Psi(t)\rangle$ as

$$|\Psi(t)\rangle = \sum_{n_1,n_2} \exp[-i\omega(n_1 + n_2)t][C_{n_1,n_2}^{+}(t)\exp(-i\omega t/2) \times |n_1, n_2, p_0 - \hbar k(n_1 - n_2), +\rangle + C_{n_1,n_2}^{-}(t)\exp(i\omega t/2) \times |n_1, n_2, p_0 - \hbar k(n_1 - n_2), -\rangle], \quad (15)$$

with $n_1, n_2 \geq 0$. This readily yields the equations of motion

$$i\hbar\frac{d}{dt}C_{n_1,n_2}^{-}(t) = \left\{\frac{1}{2M}[p_0 - \hbar k(n_1 - n_2)]^2 - \frac{1}{2}\hbar(\omega_0 - \omega)\right\}C_{n_1,n_2}^{-}(t) + \frac{\hbar\Omega_0}{2(2)^{1/2}}[n_1^{1/2}C_{n_1-1,n_2}^{+}(t) + n_2^{1/2}C_{n_1,n_2-1}^{+}(t)] \quad (16)$$

and

$$i\hbar\frac{d}{dt}C_{n_1,n_2}^{+}(t) = \left\{\frac{1}{2M}[p_0 - \hbar k(n_1 - n_2)]^2 - \frac{1}{2}\hbar(\omega_0 - \omega)\right\} \times C_{n_1,n_2}^{+}(t) + \frac{\hbar\Omega_0}{2(2)^{1/2}}[(n_1 + 1)^{1/2}C_{n_1+1,n_2}^{-}(t) + (n_2 + 1)^{1/2}C_{n_1,n_2+1}^{-}(t)]. \quad (17)$$

Instead of labeling the probability amplitudes by the photon numbers n_1 and n_2, it is convenient to introduce energy and momentum conservation explicitly by using the field-energy quantum number n and the momentum increment quantum number ν:

$$n = n_1 + n_2, \qquad \nu = n_2 - n_1. \quad (18)$$

The state vector expansion then reads

$$|\Psi(t)\rangle = \sum_{\nu,n} \exp(-i\omega n t)[C_{n,\nu}^{+}(t)\exp(-i\omega t/2)|n, \nu, +\rangle + C_{n,\nu}^{-}(t)\exp(i\omega t/2)|n, \nu, -\rangle], \quad (19)$$

where $n \geq 0$, and $-n \leq \nu \leq n$. We obtain the equations of motion directly from Eqs. (16) and (17) as

$$i\hbar\frac{d}{dt}C_{n,\nu}^{-}(t) = \left[\frac{(p_0 + \nu\hbar k)^2}{2M} - \frac{1}{2}\hbar(\omega_0 - \omega)\right]C_{n,\nu}^{-}(t) + \frac{\hbar\Omega_0}{4}[(n - \nu)^{1/2}C_{n-1,\nu+1}^{+}(t) + (n + \nu)^{1/2}C_{n-1,\nu-1}^{+}(t)] \quad (20)$$

and

$$i\hbar\frac{d}{dt}C_{n-1,\nu}^{+} = \left[\frac{(p_0 + \nu\hbar k)^2}{2M} - \frac{1}{2}\hbar(\omega_0 - \omega)\right]C_{n-1,\nu}^{+}(t) + \frac{\hbar\Omega_0}{4}[(n - \nu + 1)^{1/2}C_{n,\nu-1}^{-}(t) + (n + \nu + 1)^{1/2}C_{n,\nu+1}^{-}(t)]. \quad (21)$$

Equations (20) and (21) for running waves are formally quite similar to Eqs. (13) and (14) for a standing wave. In particular, both require only two indices to label the probability amplitudes. This might appear surprising at first, for one might expect to need three quantum numbers to specify the running-waves situation (n_1, n_2, and the transverse atomic momentum). However, this is not the case: Momentum conservation allows one to determine uniquely the photon numbers in the two counterpropagating waves once the transverse atomic momentum is known. In contrast, atomic photon exchange in a standing wave is always accompanied by symmetric momentum transfer, so that the average momentum taken up by the standing wave remains equal to zero. Consequently there is no limitation on the amount of (positive and negative) momentum that can be transferred to the atom. This is analogous to a grating of infinite mass in conventional optics. The mirrors that impose the standing-wave boundary conditions can give or take any amount of momentum. The photon number in the standing wave does not correlate with the atomic momentum. Consequently Eqs. (13) and (14) are infinitely degenerate in ν.

This physical difference between the two cases translates into a difference of the coupling coefficients: In Eqs. (13) and (14) these are independent of ν, while they depend explicitly on this quantum number in Eqs. (20) and (21). This dependence implies that the set of equations for C^{+} and C^{-} is truncated after $\nu = \pm n$; one can extract a maximum of $n\hbar k$ of momentum from a running wave with n photons.

4. NUMERICAL METHOD

The Hamiltonians H^s and H^r each conserve the total energy of field plus atoms, as expressed by the conservation of the total photon number plus atomic excitation. Therefore we consider separately a succession of Fock states with photon number n. As discussed in Ref. 12, we obtain the final result by summing these contributions weighted

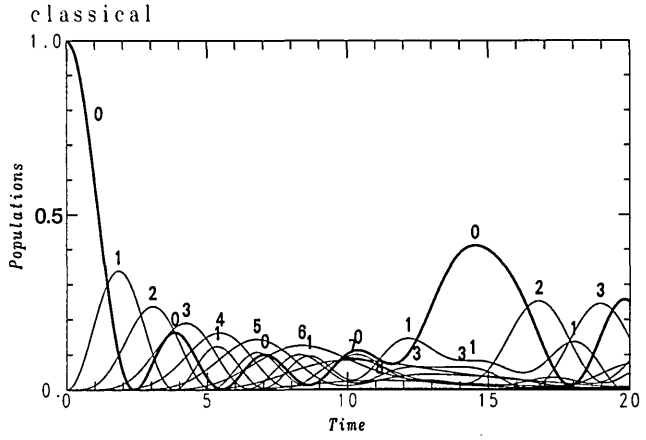

Fig. 1. Time histories of the populations $P_q(t)$ versus time in the classical regime for $\omega = \omega_0$, $\Omega_0 = 1$, $p_0 = 0$, and $\hbar k^2/2M = 0.03$. The various curves are labeled by the values of q.

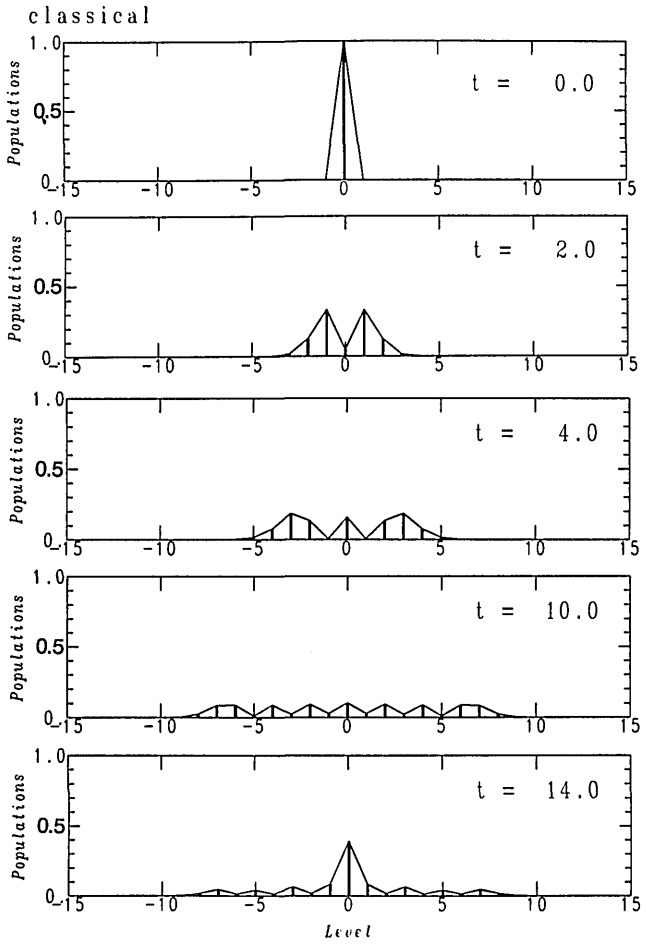

Fig. 2. Snapshots at successive times of the populations $P_q(t)$ versus q for the classical conditions of Fig. 1.

by the probability ρ_n for that photon number. We present results for coherent states with photon statistics

$$\rho_n = \exp(-\langle n\rangle)\langle n\rangle^n/n!. \tag{22}$$

For computations, it is convenient to replace Eqs. (13) and (14) by a set of equations for a single vector **A**.[14] Assuming that the atom is initially in its electronic ground state and for a given initial photon number n, we define the elements A_j to be

$$A_{2\nu}(t) = C_{n,2\nu}^{-}(t), \qquad A_{2\nu-1} = C_{n-1,2\nu-1}^{+}(t). \tag{23}$$

Rewritten in terms of this vector, Eqs. (13) and (14) become, for a given n,

$$i\frac{d}{dt}A_\nu(t) = \left[\frac{\hbar k^2}{2M}(K_0 + \nu)^2 - \frac{(-1)^\nu}{2}(\omega_0 - \omega)\right]A_\nu(t) + \frac{\Omega_0}{4}n^{1/2}[A_{\nu-1}(t) + A_{\nu+1}(t)], \tag{24}$$

where $K_0 = p_0/\hbar k$. Similarly, for the numerical solution of Eqs. (20) and (21), we define the vector **A** by the components

$$A_{2\mu}(t) = C_{n,2\nu}^{-}(t), \qquad A_{2\mu-1}(t) = C_{n-1,2\nu}^{+}(t). \tag{25}$$

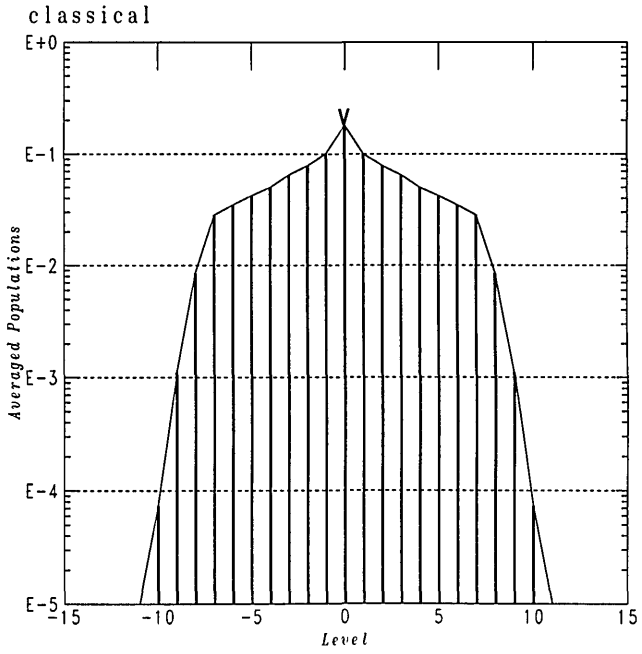

Fig. 3. Time-averaged populations $\bar{P}_q$ versus q for the classical conditions of Fig. 1. This plot, like others following, is on a logarithmic scale to show the large range of probabilities.

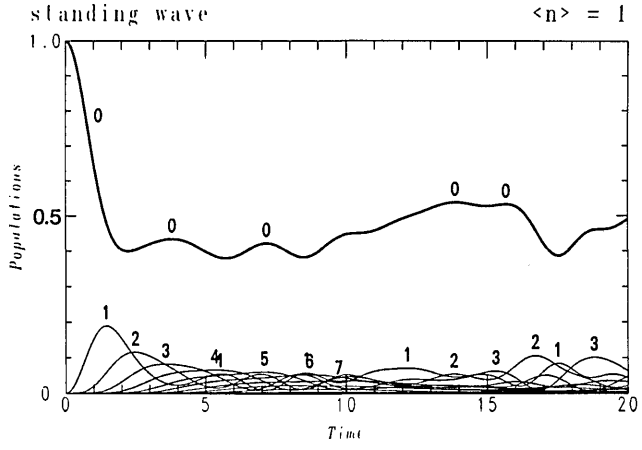

Fig. 4. Time histories of the populations $P_q(t)$ versus time in the quantum regime for a standing wave with mean photon number $\langle n\rangle = 1$ and the atomic parameters of Fig. 1.

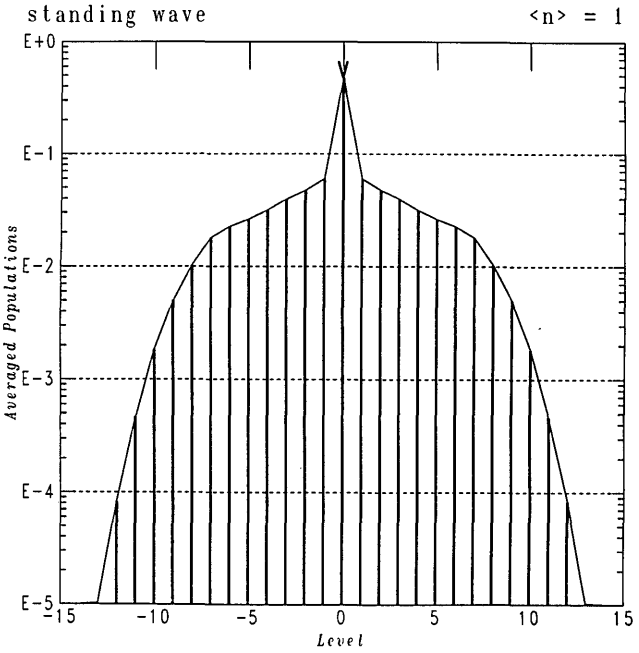

Fig. 5. Time-averaged populations $\bar{P}_q$ versus q for the standing wave of Fig. 4.

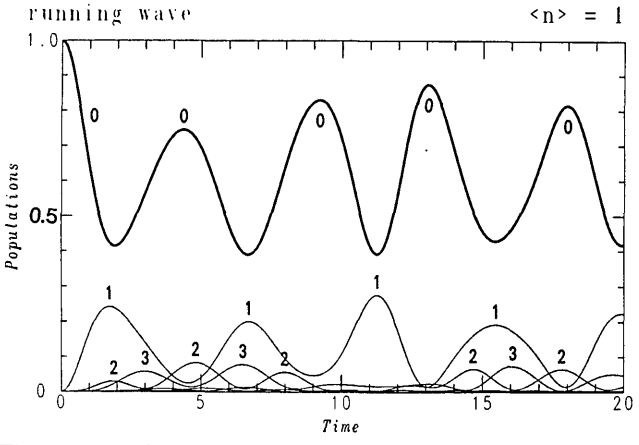

Fig. 6. Time histories of the populations $P_q(t)$ versus time in the quantum regime for counterpropagating running waves of equal amplitudes with $\langle n_1 \rangle = \langle n_2 \rangle = 0.5$ and the atomic parameters of Fig. 1.

In terms of this vector, Eqs. (20) and (21) become, for n fixed,

$$i\frac{d}{dt}A_\mu(t) = \left[\frac{\hbar k^2}{2M}(K_0 + \mu)^2 - \frac{(-1)^\mu}{2}(\omega_0 - \omega)\right]A_\mu(t) + \frac{\Omega_0}{4}[(n + \mu)^{1/2}A_{\mu-1}(t) + (n - \mu)^{1/2}A_{\mu+1}(t)]. \quad (26)$$

We see that atomic scattering is mathematically equivalent to a multistate excitation ladder, as expressed by a set of coupled ordinary differential equations whose constant coefficients form a tridiagonal matrix (of infinite dimension).[14] In the multistate excitation ladder the population is initially concentrated in one state. As time proceeds the population distribution flows into other states. The initial diffusion of population out of the initial state and into the adjacent states expresses the diffraction of the atom by the radiation field.

The general behavior of population flow in the multistate ladder is influenced by two aspects of the tridiagonal Hamiltonian: the off-diagonal elements (Rabi frequencies) tend to move population, and the diagonal elements (detunings) tend to restrict the population flow. The relative magnitudes of Ω_0 and $\hbar k^2/2M$ control the diffusion: For large k (or small mass M) the diffusion is negligible.

Under appropriate circumstances the solutions exhibit periodicities associated with the two-state Rabi oscillations between nonadjacent states. In the multistate ladder these periodicities are interpreted as multiphoton resonances, a transition in which one or more intermediate states are apparently bypassed and occur only as virtual states. In the case of atomic deflection these solutions correspond to Bragg scattering, and the periodicity corresponds to the *Pendellösung*.[10]

5. RESULTS

A. Diffraction

Figures 1–7 illustrate results for atomic diffraction in a classical standing wave, in a coherent state standing wave with mean photon number $\langle n \rangle = 1$, and in a superposition of two counterpropagating running waves of equal amplitudes and with total mean photon number $\langle n \rangle = \langle n_1 \rangle + \langle n_2 \rangle = 1$. In each case the incident atomic velocity is at a right angle to the light field, so that $p_0 = 0$, and the field frequency ω equals the Bohr frequency ω_0. Figure 1, for a classical field,[13,15–19] shows the probability that the atom has acquired transverse momentum $q\hbar k$, where q is an integer, at time t. (We use the mean quantum Rabi frequency $n^{1/2}\Omega_0$ as the classical Rabi frequency Ω.) Because the distribution of momenta about p_0 remains symmetric at all times, we plot the curves only for $q \geq 0$. For sufficiently short times (approximately $t \simeq 9$, in units of

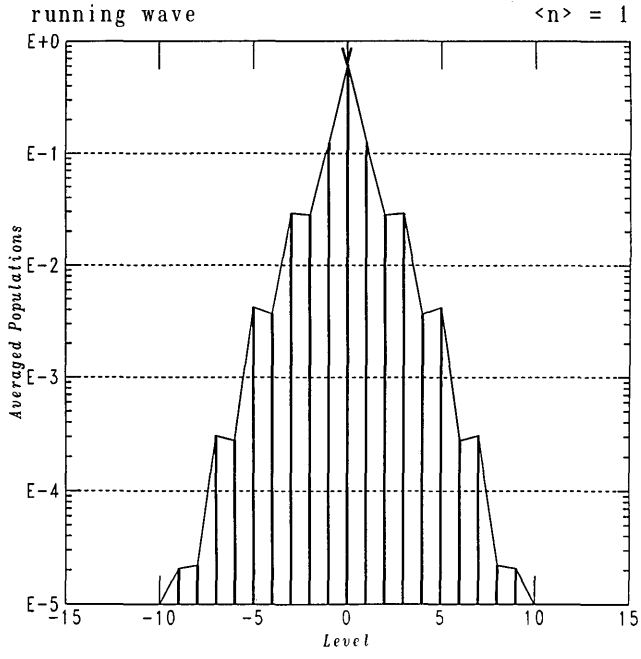

Fig. 7. Time-averaged populations $\bar{P}_q$ versus q for the traveling waves of Fig. 4.

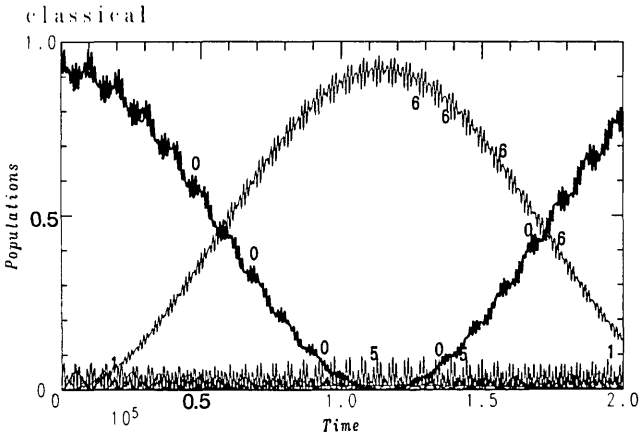

Fig. 8. Time histories of the populations $P_q(t)$ versus time in the classical regime for $\omega = \omega_0$, $\Omega_0 = 1$, $p_0 = 3\hbar k$, and $\hbar k^2/2M = 0.6$. Note the maximum time $t = 2 \times 10^5$ in this figure.

the inverse vacuum Rabi frequency), the various probabilities are given by the well-known Bessel function solutions of the Raman–Nath diffraction problem.[13,15–19] The spread of momenta is largest around $t \simeq 10$. For longer times the kinetic energy term $\hbar k^2/2M$ in Eqs. (13) and (14) becomes important, and the atomic wave function refocuses (at approximately $t \simeq 14$). This behavior is apparent in Fig. 2, which displays snapshots of the probabilities $P_q(t)$. Figure 3 shows the long-time average of these probabilities (on a logarithmic scale to show best the range of probabilities). Note that only some eight states, symmetrically placed about $p_0 = 0$, are significant in the atomic evolution.

Figure 4 is the counterpart of Fig. 1 but for a quantized standing wave. In contrast to the preceding case, here the atomic wave function remains tightly collimated in momentum space: Little population transfers to states with transverse momentum different from zero. This behavior is further illustrated in Fig. 5, which shows the long-time average populations of the atomic states with $q\hbar k$ transverse momentum. This figure differs from Fig. 3 in two ways: The central peak is higher, and the probabilities of states for $|q| > 8$ are larger. We observe a sharp peak at $q = 0$, together with a broad group of momentum states that are approximately equally populated, in a fashion quite similar to the classical case. The dominance of the $q = 0$ state, the initial state of the atom, is due to the large probability of the vacuum field, $\rho_0 = 0.368$, in a coherent state with the small mean photon number $\langle n \rangle = 1$. Because an atom in its ground electronic state does not interact with the vacuum, the probability is appreciable for the atom to remain undiffracted by the standing wave. Except for this purely quantum effect, though, the dynamics in this case resembles that of the classical regime of high quantum numbers.

Diffraction by running waves differs dramatically, as illustrated in Figs. 6 and 7. As shown in Fig. 7, only the states of transverse momentum $\pm\hbar k$ couple significantly to the initial state. The exchange between these states is nearly periodic, as illustrated in Fig. 6. A running wave initially in the one-photon number state $|1\rangle$ will be depleted as soon as it loses one quantum of momentum to the atom. Subsequently it will reabsorb this momentum from the atom. This momentum exchange occurs periodically. In a coherent state, however, there is also a probability of having two photons in the field even at small mean photon numbers. Indeed, for the case at hand with $\langle n_1 \rangle = 1/2$, we have $\rho_2/\rho_1 = 0.25$, so that the exchange of momentum is only approximately periodic.

B. Deflection

We now turn to a comparison of the effect of standing waves and running waves on atomic deflection. To exhibit the phenomena of Bragg reflection (and the subsequent *Pendellösung*) undisturbed by diffraction, we model a lighter atom (or shorter wavelength field) than in Subsection 5.A. We consider an atom whose initial transverse momentum is $3\hbar k$. As before, we take the resonant condition $\omega = \omega_0$. One would expect for the classical Hamiltonian a *Pendellösung*-type oscillation[10,20] between atomic states of transverse momenta $3\hbar k$ and $-3\hbar k$, or a net transfer of 6 quanta of transverse momentum. Figure 8 shows the classical version of such an interaction. The slow oscillation between states 0 and 6, with a period of some 2×10^5, is the *Pendellösung* oscillation. The rapid oscillations correspond to exchanges of single increments of transverse momentum. The long-time averaged populations of states of transverse momenta $q\hbar k$ shown in Fig. 9 further illustrate that the coupling is predominantly between the states with momenta $\pm 3\hbar k$.

When we employ a standing wave with low mean photon number, a noticeable change occurs in the *Pendellösung*. Figure 10 illustrates this change for a coherent-state field with mean photon number $\langle n \rangle = 1$. The difference between Figs. 10 and 8 is due to the probability of the vacuum state as one component of the coherent state. Figure 11, the quantum counterpart of Fig. 9, shows quite clearly the vacuum increment that is added to the initial state. For mean photon numbers as low as $\langle n \rangle \simeq 5$, the population of the vacuum state becomes negligible, and we recover the symmetry of the classical results. The situation is quantitatively different when we try to deflect the

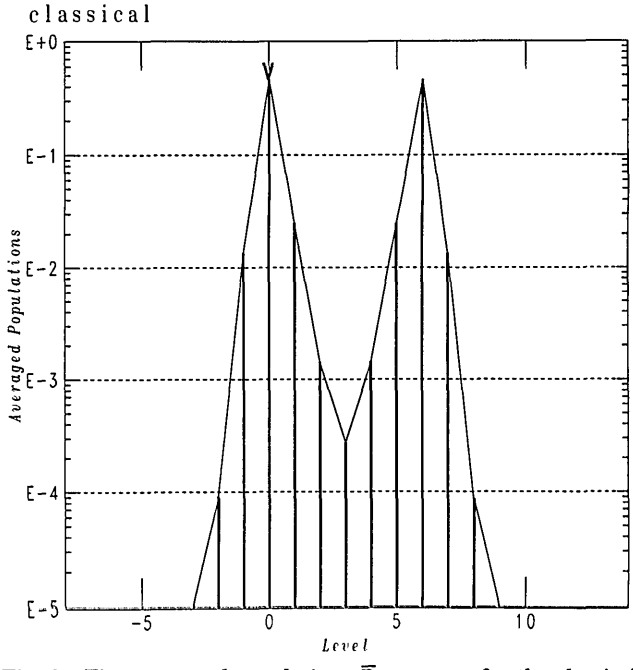

Fig. 9. Time-averaged populations $\overline{P}_q$ versus q for the classical conditions of Fig. 8.

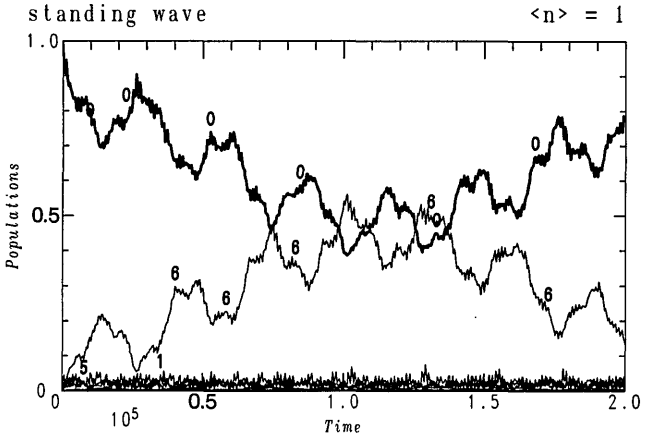

Fig. 10. Time histories of the populations $P_q(t)$ versus time in the quantum regime for a standing wave with mean photon number $\langle n \rangle = 1$ and the atomic parameters of Fig. 8. Note the maximum time $t = 2 \times 10^5$ in this figure.

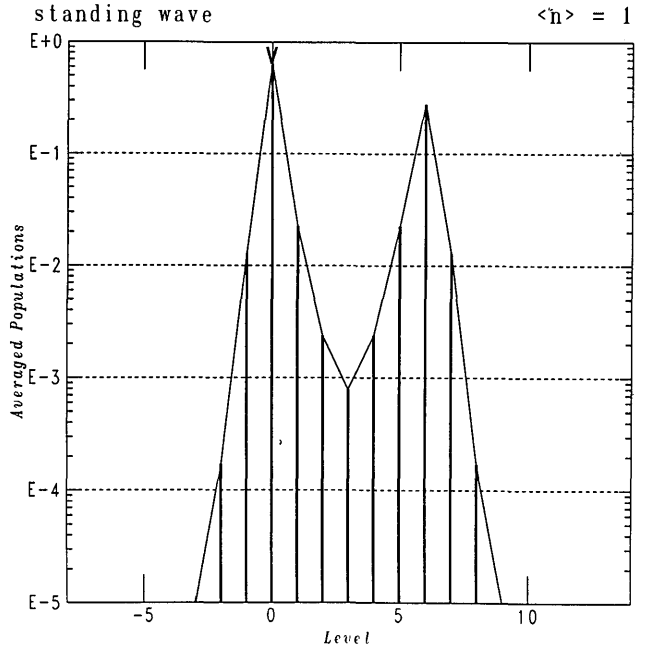

Fig. 11. Time-averaged populations $\overline{P}_q$ versus q for the conditions of Fig. 10.

atom by two counterpropagating running waves. For the low mean photon numbers considered here, the running wave cannot provide the $6\hbar k$ of transverse momentum necessary to couple the $3\hbar k$ and $-3\hbar k$ states, and the *Pendellösung* disappears altogether. The time-averaged population shows only a single peak, as in Fig. 12. More surprising is the fact that the *Pendellösung* solution still disappears for a mean photon number as large as $\langle n \rangle = 100$, as illustrated in Fig. 13. This absence of Bragg deflection can be understood on physical grounds: The creation of an imbalance between the numbers of photons in the forward and the backward waves breaks the spatial periodicity that produces Bragg scattering in a periodic grating such as a standing wave.

We can also apply our experience with multiphoton resonance to obtain an intuitive feeling for the difference between standing and running waves, even for the case of a photon-number state. Perturbation theory may be used to calculate the period of a multiphoton resonance: It is the product of a succession of diagonal elements of the Hamiltonian (detunings) divided by a product of off-diagonal elements (Rabi frequencies). Perturbation theory also predicts a shift in the position of the resonance. The conditions needed for multiphoton resonance become more constraining as the order of the process becomes larger: The period becomes longer, and the multistep detuning must be more sharply fixed.

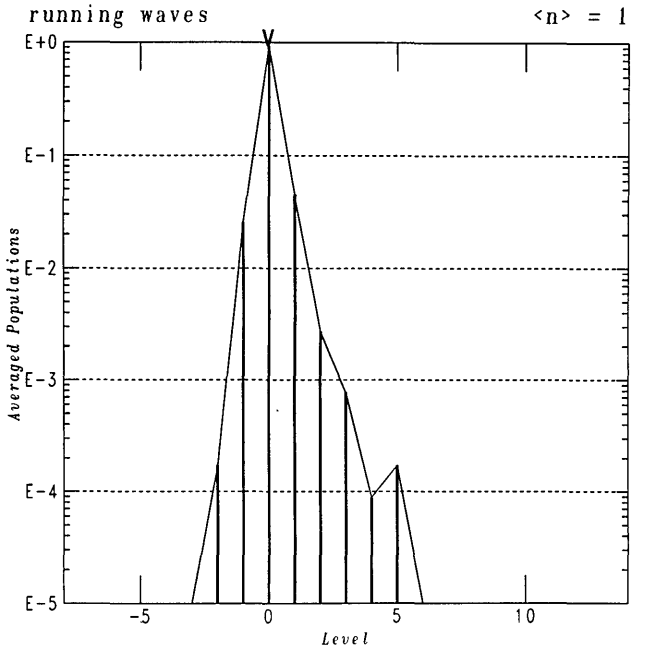

Fig. 12. Time-averaged populations $\overline{P}_q$ versus q for counterpropagating running waves of equal amplitudes with $\langle n_1 \rangle = \langle n_2 \rangle = 0.5$ and the atomic parameters of Fig. 8.

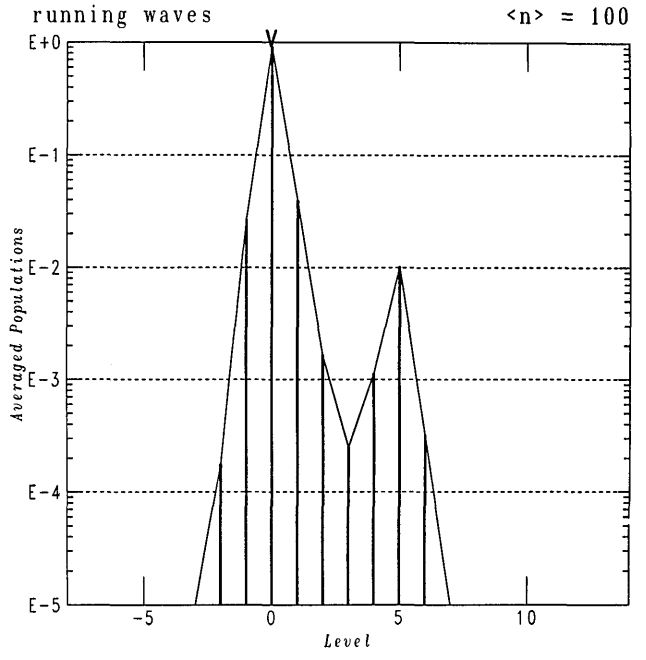

Fig. 13. Time-averaged populations $\overline{P}_q$ versus q for counterpropagating running waves of equal amplitudes with $\langle n_1 \rangle = \langle n_2 \rangle = 50$ and the atomic parameters of Fig. 8.

Applying these results to the problem at hand, we note that for a field in a number state the tridiagonal matrix derived from the standing-wave Hamiltonian has a uniform distribution of Rabi frequencies. The matrix derived for the running waves, in contrast, has a variation of Rabi frequencies. The result of this variation is a shift in the location of the multiphoton resonance. As a consequence of this subtle quantum effect, the sharp multiphoton resonances that occur with standing waves are not found with running waves until the photon number becomes extremely large. The larger the deflection, the larger must be the photon number. For the case of Fig. 13, which involves a deflection of $6\hbar k$, the photon number must be of the order of 10^3 before the *Pendellösung* becomes possible.

6. CONCLUSIONS

The mathematical difference between a single-mode standing wave and the equivalent pair of running waves manifests itself only in the coupling matrix elements of Eqs. (13) and (14) or Eqs. (20) and (21). These differences follow directly from the quantization procedure for the normal modes of the electromagnetic field. A choice of eigenmodes embodies a decision about the character of the state we create by the operator $a^\dagger$. Our choice determines the energy and momentum carried by the field increments, the photons. Different choices make energy and momentum conservation manifest themselves differently. Superficially, the change of basis states merely introduces a linear transformation of the creation operator, but when the system is coupled to a set of atoms that can probe the structure of the modes, momentum conservation allows us to infer the physical boundary conditions of the electromagnetic field. The momentum increments acquired by the atoms must match those available from the field. Two independently imposed traveling waves offer a limited amount of momentum, whereas the mirrors that establish and maintain a stable standing-wave structure serve as inexhaustible momentum sources and sinks.

A similar interpretation is also available in a semiclassical description of the field–atom interaction. If we properly consider the energy–momentum exchange, we can selectively absorb one traveling-wave component, e.g., by Doppler shifting the atomic transition into resonance with it.[21] However, if the two waves are generated by reflection in a standing-wave cavity, the change of field amplitude will be distributed over both waves within a few cavity round-trip times. This reestablishes the standing-wave pattern. Thus the atomic behavior can, also in this case, be described as a scattering process from a rigid lattice. It should be noted that our quantum treatment, based on a single-cavity mode, implicitly requires that we consider phenomena that occur over time scales much longer than the cavity round-trip time.

ACKNOWLEDGMENTS

The research of B. W. Shore is performed under the auspices of the U.S. Department of Energy at Lawrence Livermore National Laboratory under contract W-7405-Eng-48. That of P. Meystre is supported by the U.S. Office of Naval Research under contract N00014-88-K-0294 and by NSF grant PHY-8902548. The research of S. Stenholm was supported in part by the Joint Services Optics Program. We have benefited from clarifying discussions with C. Cerjan, M. Sargent III, M. Wilkens, and E. M. Wright.

P. Meystre is also with the Department of Physics, University of Arizona, Tucson, Arizona 85721.

*Permanent address, Research Institute for Theoretical Physics, University of Helsinki, Siltavuorenpenger 20C, SF-00170 Helsinki 17, Finland.

REFERENCES

1. For a recent tutorial review, see V. I. Balykin and V. S. Lethokov, "Laser optics of neutral atomic beams," Phys. Today **42** (4), 23 (1989).
2. R. Ya. Dubetsky, A. P. Kazantsev, V. P. Chebotayev, and V. P. Yakovlev, "Interference of atoms and formation of atomic spatial arrays in light fields," Pis'ma Zh. Eksp. Teor. Fiz. **39,** 649 (1984) [JETP Lett. **39,** 649 (1984)]; V. P. Chebotayev, R. Ya. Dubetsky, A. P. Kazantsev, and V. P. Yakovlev, "Interference of atoms in separated optical fields," J. Opt. Soc. Am. B **2,** 1791 (1985).
3. J. F. Clauser, "Ultra-high sensitivity accelerometers and gyroscopes using neutral atom matter–wave interferometry," Physica B **151,** 262 (1988).
4. E. Arimondo, H. Lew, and T. Oka, "Deflection of a Na beam by resonant standing-wave radiation," Phys. Rev. Lett. **43,** 753 (1979).
5. P. E. Moskowitz, P. L. Gould, S. R. Atlas, and D. E. Pritchard, "Diffraction of an atomic beam by standing-wave radiation," Phys. Rev. Lett. **51,** 370 (1983).
6. J. W. Early, "Deflection of barium atoms by a standing-wave light field," Opt. Commun. **65,** 250 (1988).
7. P. L. Gould, G. A. Ruff, and D. E. Pritchard, "Diffraction of atoms by light: the near-resonant Kapitza–Dirac effect," Phys. Rev. Lett. **56,** 827 (1986).
8. C. Salomon, J. Dalibard, A. Aspect, H. Metcalf, and C. Cohen-Tannoudji, "Channeling atoms in a laser standing wave," Phys. Rev. Lett. **59,** 1659 (1987).
9. P. J. Martin, P. L. Gould, B. G. Oldaker, A. H. Miklich, and D. E. Pritchard, "Diffraction of atoms moving through a standing light wave," Phys. Rev. A **36,** 2495 (1987).
10. P. J. Martin, B. G. Oldaker, A. H. Miklich, and D. E. Pritchard, "Bragg scattering of atoms from a standing light wave," Phys. Rev. Lett. **60,** 515 (1988).
11. For a recent tutorial review, see S. Haroche and D. Kleppner, "Cavity QED," Phys. Today **42**(1), 24 (1989).
12. See, e.g., P. Meystre, E. Schumacher, and S. Stenholm, "Atomic beam deflection in a quantum field," Opt. Commun. **73,** 443 (1989).
13. A. F. Bernhardt and B. W. Shore, "Coherent atomic deflection by resonant standing waves," Phys. Rev. A **23,** 1290 (1981).
14. B. W. Shore, *The Theory of Coherent Atomic Excitation* (Wiley Interscience, New York, 1990).
15. R. J. Cook and A. F. Bernhardt, "Deflection of atoms by a resonant standing electromagnetic wave," Phys. Rev. A **18,** 2533 (1978).
16. G. A. Delone, V. A. Grinchuk, S. D. Kuzmichev, M. L. Nagavea, A. P. Kazantsev, and G. I. Surdutovich, "Scattering of atoms and molecules by an electromagetic field," Opt. Commun. **33,** 149 (1980).
17. E. Arimondo, A. Bambini, and S. Stenholm, "Quasiclassical theory of laser-induced atomic-beam dispersion," Opt. Commun. **37,** 103 (1981); Phys. Rev. A **24,** 898 (1981).
18. C. Tanguy, S. Reynaud, and C. Cohen-Tannoudji, "Deflection of an atomic beam by a laser wave: transition between diffractive and diffusive regimes," J. Phys. B. **17,** 4623 (1984).
19. A. P. Kazantsev, G. A. Ryabenko, G. I. Surdovich, and V. P. Yakovlev, "Scattering of atoms by light," Phys. Rep. **129,** 77 (1985).
20. P. Meystre, E. Schumacher, and E. M. Wright, "Quantum Pendellösung in atom diffraction by a light field," Ann. Phys. (Leipzig), to be published.
21. See, e.g., P. Meystre and M. Sargent III, *Elements of Quantum Optics* (Springer-Verlag, New York, 1990).